Supporting Information

Montgomery et al. 10.1073/pnas.1720940115

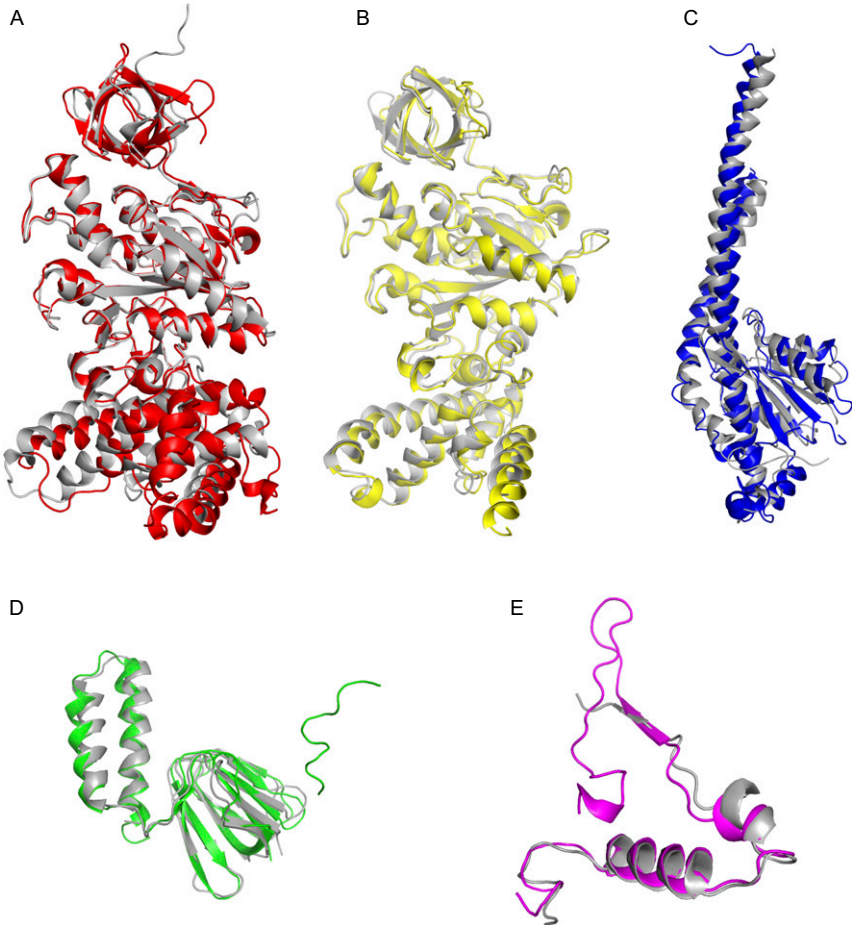

Fig. S1. Comparison of individual subunits of the F_1-ATPase from *T. brucei* with orthologs in the bovine F_1-ATPase inhibited by dicyclohexylcarbodiimide (12). The *T. brucei* subunits are colored, and bovine subunits are in gray. (*A*) The α_{DP}-subunit (red; rmsd 2.3 Å). (*B*) The β_{DP}-subunit (yellow; rmsd 2.0 Å). (*C*) The γ-subunit (blue; rmsd 3.8 Å). (*D*) The δ-subunit (green; rmsd 2.1 Å). (*E*) The ε-subunit (magenta; rmsd 1.8 Å).

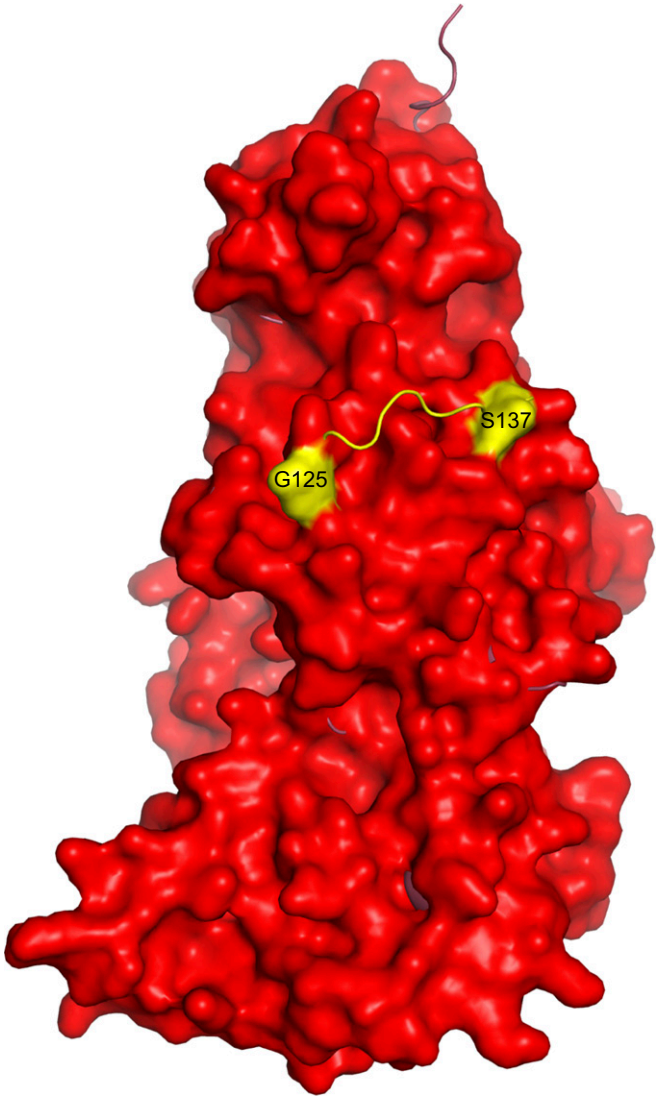

Fig. S2. The sites of proteolytic cleavage in the α-subunits of the F_1-ATPase from *T. brucei*. Shown is a cartoon representation of the α_{DP}-subunit from *T. brucei*, in surface representation, overlaid onto the equivalent subunit from the bovine enzyme inhibited by dicyclohexylcarbodiimide (12) (mainly hidden by the *T. brucei* surface). The proteolytic cleavages in the *T. brucei* subunit follow residues 127 and 135, removing 128–135. Residues G125 and S137 are in yellow. The equivalent region in the bovine α_{DP}-subunit, residues 117–123, is not cleaved by proteolysis and forms a solvent-exposed loop in yellow.

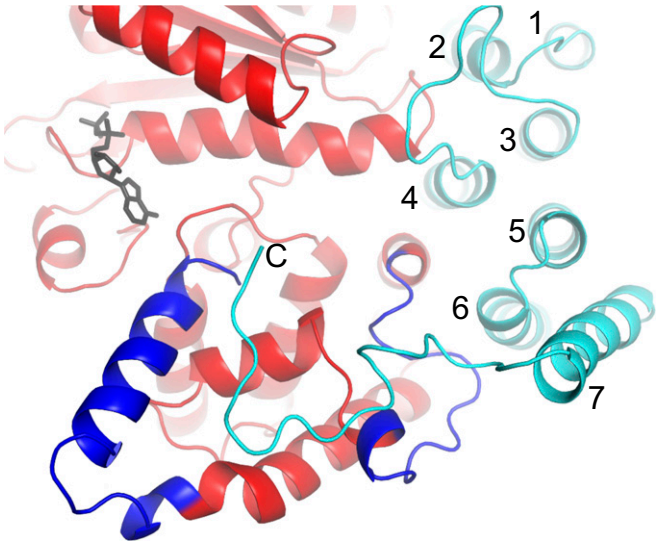

Fig. S3. The roles of the additional segments of the sequences in the α-subunits of the F_1-ATPase from *T. brucei*. The parts of the nucleotide-binding and C-terminal domains of the α_E-subunit that interact with the p18-subunit (cyan) are shown in red, except for the additional segments (residues 483–498 and 536–560), which are in royal blue for emphasis. A bound ADP molecule is in black. The α-helices in subunit p18 are numbered 1–7.

```
      18  -TNTAPWIEKIKKCKYYDEAGEVLVNMNVSNCPPDI--  52
p18   57  -ATLQCIYQSPSKQSTPVDNESKFCAMMDLLEEMQH--  91
     100 -ESWTWVMKECVKSGQFRLGYCIQQVMETECKGCPA-- 142
         --TYNALINAYAK-G--EEA--LY--M---G--PN---   PPRcon
      71  -SALEMVVRALGREGQHDAVCALLDETPLPPGSRLD-- 105
     107 -RAYTTVLHALSRAGRYERALELFAELRRQGVAPTL-- 141
     142 -VTYNVVLDVYGRMGRSWPRIVALLDEMRAAGVEPD-- 176
     178 -FTASTVIAACSRDGLVDEAVAFFEDLKARGHAPSV-- 212
     213 -VTYNALLQVFGKAGNYTEALRVLGEMEQNGCQPDA-- 247
     248 -VTYNELAGTYARAGFFEEAARCLDTMASKGLLPNA-- 282
     283 -FTYNTVMTAYGNVGKVDEALALFDQMKKTGFVPNV-- 317
     318 -NTYNLVLGMLGKKSRFTVMLEMLGEMSRSGCTPNR-- 352
PPR10 353 -VTWNTMLAVSGKRGMEDYVTRVLEGMRSSGVELSR-- 387
     388 -DTYNTLIAAYGRCGSRTNAFKMYNEMTSAGFTPCI-- 422
     423 -TTYNALLNVLSRQGDWSTAQSIVSKMRTKGFKPNE-- 457
     458 -QSYSLLLQCYAKGGNVAGIAAIENEVYGSGAVFPS-- 492
     494 -VILRTLVIANFKCRRLDGMETAFQEVKARGYNPDL-- 528
     529 -VIFNSMLSIYAKNGMYSKATEVFDSIKRSGLSPDL-- 563
     564 -ITYNSLMDMYAKCSESWEAEKILNQLKCSQTMKPD-- 598
     600 -VSYNTVINGFCKQGLVKEAQRVLSEMVADGMAPCA-- 634
     635 -VTYHTLVGGYSSLEMFSEAREVIGYMVQHGLKPME-- 669
     670 -LTYRRVVESYCRAKRFEEARGFLSEVSETDLDFDK-- 704
```

Fig. S4. Comparison of the PPR sequences in the p18-subunit of the F_1-ATPase from *T. brucei* and the 18 PPRs in the PPR10 protein from *Z. mays* with the PPR consensus sequence (red) (56). The sequences of the four PPR10 domains used in the structural comparison shown in Fig. 3 are in blue. The PPRs in subunit p18 were predicted with TPRpred (73). The alignment was produced manually.

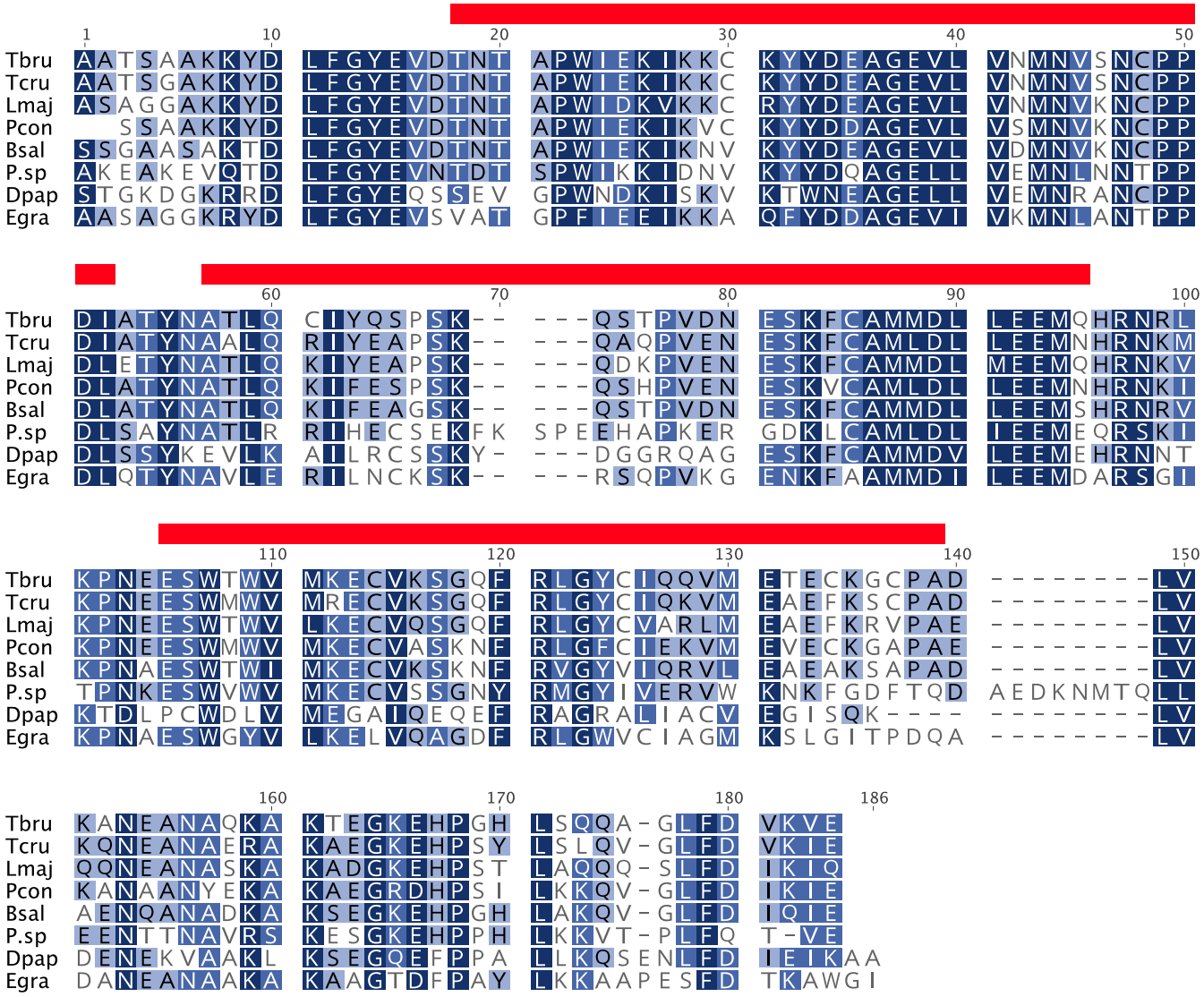

Fig. S5. Conservation of sequences of p18-subunits of ATP synthases from euglenozoa. Bsal, *Bodo saltans*; Dpap, *Diplonema papillatum*; Egra, *Euglena gracilis*; Lmaj; *Leishmania major*; Pcon, *Paratrypanosoma confusum*; P. sp, *Perkinsela sp*; Tbru, *T. brucei*; Tcru, *Trypanosoma cruzi*. Identities and conservative substitutions are shown in dark blue and light blue, respectively. The red bars indicate the PPR domains predicted by TPRpred (73).

Table S1. Data collection and refinement statistics for the F_1-ATPase from *T. brucei*

Parameter	Value
Space group	$P2_1$
Unit cell dimensions a, b, c, Å; β	124.2, 206.3, 130.2; 104.9°
Resolution range, Å	3.20–90.51
High-resolution bin, Å	3.20–3.25
No. of unique reflections	102,391 (5,076)
Multiplicity	3.5 (3.7)
Completeness, %	98.2 (97.6)
R_{merge}*	0.123 (0.565)
<I/σ (I)>	8.1 (2.8)
B factor, from Wilson plot, Å^2	46.5
R factor†, %	27.2
R_{free}‡, %	29.7
rmsd of bonds, Å	0.007
rmsd of angles, °	1.07

Statistics for the highest-resolution bin are in parentheses.

*$R_{merge} = \sum_h \sum_i |I(h) - I(h)_i| / \sum_h \sum_i I(h)_i$, where $I(h)$ is the mean weighted intensity after rejection of outliers.

†R factor $= \sum_{hkl} ||F_{obs}| - k|F_{calc}|| / \sum_{hkl} |F_{obs}|$, where F_{obs} and F_{calc} are the observed and calculated structure factor amplitudes, respectively.

‡$R_{free} = \sum_{hkl \subset T} ||F_{obs}| - k|F_{calc}|| / \sum_{hkl \subset T} |F_{obs}|$, where F_{obs} and F_{calc} are the observed and the calculated structure factor amplitudes, respectively, and T is the test set of data omitted from refinement.

Table S2. Buried surface areas of catalytic interfaces in selected structures of F_1-ATPases

	Buried surface area of catalytic interface, Å^2		
Structure	Diphosphate	Triphosphate	Empty
T. brucei	2,300	2,400	1,900
S. cerevisiae (PDB ID code 2HLD; molecule 1)	2,000	2,300	1,900
Bovine phosphate release dwell (PDB ID code 2JDI)	3,000	2,200	1,900
Bovine catalytic dwell (PDB ID code 4ASU)	2,500	2,200	1,800
Bovine inhibited with ADP-AlF_4 (PDB ID code 1H8E)	2,800	2,100	2,300
C. thermarum wild type (PDB ID code 5HKK)	2,900	2,000	1,900